PERGAMON

Pattern Recognition 35 (2002) 199–210

PATTERN RECOGNITION
THE JOURNAL OF THE PATTERN RECOGNITION SOCIETY

www.elsevier.com/locate/patcog

A pseudo top-hat mathematical morphological approach to edge detection in dark regions

T. Chen[a], Q.H. Wu[a,*], R. Rahmani-Torkaman[b], J. Hughes[b]

[a]*Department of Electrical Engineering and Electronics, The University of Liverpool, Liverpool, L69 3GJ, UK*
[b]*Manufacturing Systems Engineering Technology, BICC General UK Cables Limited, Wrexham, LL13 9PH, UK*

Received 12 November 2000; accepted 30 November 2000

Abstract

Edge detection is an important pre-processing step in image segmentation. Conventionally, edges are detected according to gradient property, then processed by the thresholding technique. By such an approach, fine edge details in dark region of the image are eliminated. It is annoying sometimes as they are as useful as those in bright region, although this is caused by unevenly distributed lighting in many machine vision applications. In this paper, a novel mathematical morphological edge detection algorithm, based on pseudo top-hat transformation which is derived from top-hat transformation, is proposed to preserve these edge details as well as prominent ones. The algorithm is also presented in detail. Comprehensive experimental results show that the proposed algorithm is efficient for edge details extraction in place of shading while preserving distinguish features.

Keywords: Edge detection; Threshold; Quad-tree decomposition; Mathematical morphology; Top-hat transformation

1. Introduction

Edge detection is an essential preliminary step in image segmentation. An edge is the boundary where distinct intensity changes or discontinuities occur. Edge detection is a process which transforms a grey-level image to an edge image, which indicates either the presence or absence of an edge [1]. Derivative edge detectors are straightforward methods for edge detection [2]. The first-order differential operators such as Robert, Sobel operators are convolved with images to enhance spatial intensity changes, then a threshold is applied to obtain edge points. The second-order differential operator such as Laplacian operator, indicates edge points by its zero-crossing property [2,3]. Other edge detectors such as Prewitt operator [2] try to fit a least-squares-error quadratic surface over a 3×3 image window and differentiate the fitted surface. This is named template matching operator. Template matching operators are superior to the simple derivative operators, especially as noise increases.

Mathematical morphology provides an alternative approach to image processing based on shape concept stemmed from set theory [4]. In the mathematical morphology theory, images are treated as sets, morphological transformations derived from Minkowski addition and subtraction are defined to extract features in images. As the performance of classic edge detectors degrades with noise, morphological edge detector has been studied [5]. Blur-minimum and α-trimmed mean morphological edge detectors [5,6] have been proposed to detect edges without bias under noise interference conditions. Studies show that morphological edge detectors have outperformed previous edge detectors in robustness of detecting edges with presence of noise.

As a ubiquitous technique in image segmentation, thresholding is usually applied as post-processing of edge detection to obtain edge points. Various threshold methods have been proposed for image segmentation.

* Corresponding author. Tel.: + 44-151-7944535; fax: + 44-151-7944540.
E-mail address: q.h.wu@liverpool.ac.uk (Q.H. Wu).

0031-3203/01/$20.00
PII: S0031-3203(01)00024-3

Applied it to edge detection, a global threshold value is normally chosen to threshold the whole image into binary one. For Canny edge detector [7], it was suggested that thresholding be conducted using hysteresis rather than simply selecting a threshold value to apply everywhere. Although these thresholding methods perform well in extracting distinguishable edges, the tiny grey-level changes in dark regions are always shaded away. Sometimes they are actually critical features interested by observer, particularly in machine vision applications, when lighting is not evenly distributed on objects as ideally expected. This demands edge detection algorithm distinguish small grey-level changes as well as preserving prominent grey-level changes in different regions. Within these regions augmented distinction of small grey-level changes are able to be extracted as edge features by different threshold values determined by certain criteria in each region.

In this paper, a novel mathematical morphology edge detection algorithm is proposed to extract smooth edge features in dark regions. As an extension of basic mathematical morphological operators, top-hat transformation sharpens small grey-level changes in place of shading. But the distinction is not augmented enough to threshold small grey-level edge changes. As there are invariant pixels under opening(closing) transformation of image, pseudo top-hat transformation (PTHT) is defined. It subtracts original image with invariant pixels set image, which augments small grey-level changes. The result image is then decomposed into subimages by recursive quad-tree decomposition scheme, and different threshold values are determined by certain criteria in each subimage to obtain edge image. This paper is organized as follows. Section 2 presents definitions of mathematical morphological operations and their extensions as morphological edge detector and top-hat transformation. Section 3 proposes pseudo top-hat transformation based on invariant pixels under opening(closing) transformation. Details of the algorithm are discussed in Section 4. Section 5 presents comprehensive comparisons between PTHT edge detection algorithm with existing edge detection methods. Comparisons on computation time and memory requirements of different edge detection methods are given in Section 6. Section 7 concludes our discussion.

2. Mathematical morphological operators

Mathematical morphology theory is developed from geometry. It was introduced by Matheron [4] as a technique for analyzing geometric structure of metallic and geologic samples. It was extended to image analysis by Serra [4]. Based on set theory, mathematical morphology is established by introducing fundamental operators applied to two sets. One set is said to be processed by another which is known as structuring element. Let I denote a grey-scale two dimensional image, B denote structuring element. The basic mathematical morphological operators are dilation and erosion, derived from these, opening and closing operations are also defined.

Dilation of a grey-scale image $I(x, y)$ by a grey-scale structuring element $B(s, t)$ is denoted by

$$(I \oplus B)(x, y) = \max\{I(x - s, y - t) + b(s, t)\}. \quad (1)$$

The domain of $I \oplus B$ is the dilation of the domain of I by the domain of B.

Erosion of a grey-scale image $I(x, y)$ by a grey-scale structuring element $B(s, t)$ is denoted by

$$(I \ominus B)(x, y) = \min\{I(x + s, y + t) - b(s, t)\}. \quad (2)$$

The domain of $I \ominus B$ is the erosion of the domain of I by the domain of B.

Opening of a grey-scale image $I(x, y)$ by a grey-scale structuring element $B(s, t)$ is denoted by

$$I \circ B = (I \ominus B) \oplus B. \quad (3)$$

Closing of a grey-scale image $I(x, y)$ by a grey-scale structuring element $B(s, t)$ is denoted by

$$I \bullet B = (I \oplus B) \ominus B. \quad (4)$$

Dilation is the maximum pixels set union when structuring element overrides image, while erosion is the minimum pixels set union when image is overlapped by structuring element. Dilation expands image set and erosion shrinks it. Opening is erosion followed by dilation and closing is dilation followed by erosion. Opening generally smoothes the contour of an image, breaks narrow gaps. As opposed to opening, closing tends to fuse narrow breaks, eliminates small holes, and fills gaps in the contours.

The edge of image I, denoted by $E_d(I)$, is defined as the difference set of the dilation domain of I and the domain of I. This is also known as dilation residue edge detector:

$$E_d(I) = (I \oplus B) - I. \quad (5)$$

Equivalently, the edge of image I, denoted by $E_e(I)$, can also be defined as the difference set of the domain of I and the erosion domain of I. This is also known as erosion residue edge detector:

$$E_e(I) = I - (I \ominus B). \quad (6)$$

The opening top-hat transformation of image I, denoted as $TH_o(I)$, is defined as the difference set of the domain of I and the opening domain of I. It is defined as

$$TH_o(I) = I - (I \circ B). \quad (7)$$

Similarly, the closing top-hat transformation of image I, denoted as $TH_c(I)$, can also be defined as the difference set of the closing domain of I and the domain of I. It is defined as

$$TH_c(I) = (I \bullet B) - I. \quad (8)$$

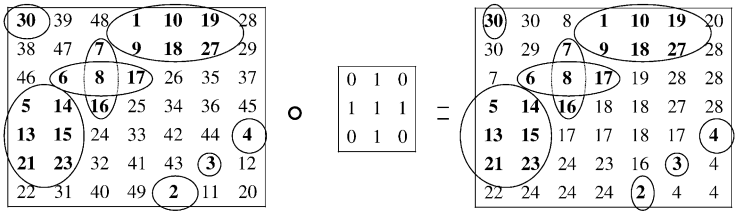

(a) (b) (c)

Fig. 1. Invariant pixels under opening operation by binary structuring element. (a) Grey-scale image. (b) Structuring element. (c) Opening result of grey-scale image (a).

3. Pseudo top-hat transformation

In order to identify the feature of images, a concept of 'invariant pixels' is introduced based on the binary structuring elements. Under opening and closing operations, there are some pixels which are invariant in an image. They can be identified by the following propositions.

Proposition 1. *A pixel is invariant under opening if and only if it is the local minimum value pixel in the neighborhood of the structuring element. That is, let* $\hat{I}$ *denote the region in image* I*, which is overlaid by the structuring element to be eroded, and if* $I(u,v) = \min(\hat{I})$*, then* $(I \circ B)(u,v) = I(u,v)$.

Proof. Let $\hat{I}$ denote the region which is overlaid by the structuring element to be eroded, I_b denote the structuring element, $\hat{I}_1$ denote the same eroded region. If $I(u,v) = \min(\hat{I})$, then according to definition of Eq. (2), erosion of I is the minimum value of this region, that is, $\hat{I}_1(u,v) = \min\{\hat{I} - I_b\}$. According to the definition of closing, erosion is followed by dilation, which takes the maximum value of interested region. In the region $\hat{I}_1$, $I(u,v)$ is always greater than any other pixels in neighborhood, which means it remains unchanged in dilation operation. Thus, $(I \circ B)(u,v) = I(u,v)$. Conversely, if $(I \circ B)(u,v) = I(u,v)$, suppose that $I(u,v)$ is in the region $\hat{I}$, which it's eroded from, then it must satisfy that $I(u,v) = \min(\hat{I})$.

Proposition 2. *A pixel is invariant under closing if and only if it is the local maximum value pixel in the neighborhood of the structuring element. That is, let* $\hat{I}$ *denote the region which is overlaid by the structuring element to be dilated, if* $I(u,v) = \max(\hat{I})$*, then* $(I \bullet B)(u,v) = I(u,v)$.

Proof. Let $\hat{I}$ denote the region which is overlaid by the structuring element to be dilated, I_b denote the structuring element, $\hat{I}_2$ denote the same dilated region. If $I(u,v) = \max(\hat{I})$, then according to the definition of Eq. (1), the dilation of I is the maximum value of this region, that is, $\hat{I}_2 = \max\{\hat{I} + I_b\}$. According to the definition of closing, dilation is followed by erosion, which takes the minimum of interested region. In the region $\hat{I}_2$, $I(u,v)$ is always less than any other pixels in neighborhood, which means it remains unchanged in erosion operation. Thus, $(I \bullet B)(u,v) = I(u,v)$. Conversely, if $(I \bullet B)(u,v) = I(u,v)$, suppose that $I(u,v)$ is in the region $\hat{I}$, which is it's dilated from, then it must satisfy $I(u,v) = \max(\hat{I})$.

As indicated in the above propositions, local minimums and local maximums are invariant under opening and closing transformations by binary structuring element, respectively. As illustrated in Fig. 1, pixel values in circles remain unchanged after opening operation. The result of opening(closing) operation consists invariant pixels in some specific locations of the image.

This leads to an alternative definition of top-hat transformation. Instead of subtracting opening set of original image from original image set, invariant pixels set under opening(closing) transformation is subtracted from original image set, small grey-level changes in image will then be augmented. Pseudo top-hat transformation is therefore defined as follows:

Definition. Let I denote an image set, I_{io} denote the invariant pixels set under opening transformation, then pseudo opening top-hat transformation, denoted by $PTH_o(I)$, is defined as

$$PTH_o(I) = I - I_{io}. \tag{9}$$

Definition. Let I denote an image set, I_{ic} denote the invariant pixels set under closing transformation, then pseudo closing top-hat transformation, denoted by $PTH_c(I)$, is defined as

$$PTH_c(I) = I_{ic} - I. \tag{10}$$

Comparing with top-hat transformation which distinguishes small grey-level changes in place of shading as shown in Fig. 2, pseudo top-hat transformation augments small grey-level changes as well as prominent grey-level changes as illustrated in Fig. 3. As shown in

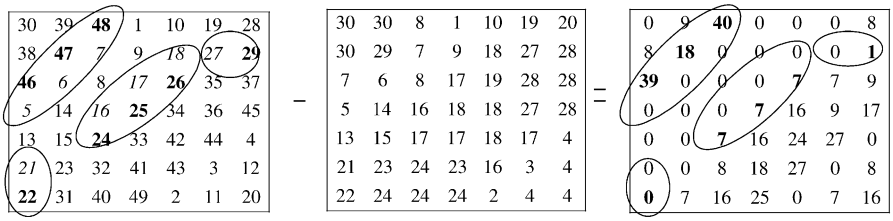

Fig. 2. Opening top-hat transformation illustration. (a) Grey-scale image. (b) Opening transformation. (c) Opening top-hat transformation result of (a).

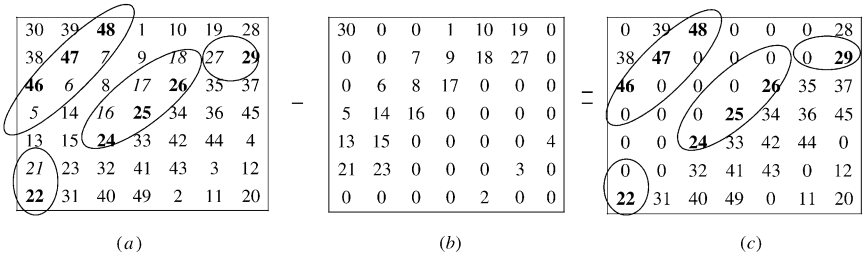

Fig. 3. Pseudo opening top-hat transformation illustration. (a) Grey-scale image. (b) Invariant pixels set under opening transformation. (c) Pseudo opening top-hat transformation result of (a).

Fig. 2(a), there are two double pairs as 21–22 and 27–29 that grey-level changes are very small in bottom left corner and top right corner circles. They are transformed by opening top-hat transformation, results are 0–0 and 0–1, respectively, as shown in Fig. 2(c). Small grey-level changes are not distinguished to be thresholded to indicate possible edge points. There are two triple pairs in Fig. 2(a), one is 46–47–48/5–6–7, which is a prominent grey-level change, the other is 24–25–26/16–17–18, which is a rather smooth grey-level change. They are transformed by opening top-hat transformation, results are 39–18–40/0–0–0 and 7–7–7/0–0–0, respectively, as shown in Fig. 2(c). The prominent change is distinguished, though the smooth grey-level change is not augmented to be prominent. As shown in Fig. 3(a), two double pairs 21–22 and 27–29 are transformed by pseudo top-hat transformation, results are 0–22 and 0–29, respectively, as shown in Fig. 3(c). The small grey-level changes are augmented and distinguished significantly. Two triple pairs 46–47–48/5–6–7 and 24–25–26/16–17–18 as shown in Fig. 3(a), are transformed by pseudo top-hat transformation, results are 46–47–48/0–0–0 and 24–25–26/0–0–0, respectively, as shown in Fig. 3(c). The prominence grey-level change as well as the small grey-level change are both distinguished to be prominent changes.

4. The proposed algorithm

4.1. General description

A novel algorithm is presented to detect edges in dark regions as well as preserve feature edges in bright regions. The image is first processed by a morphological residue edge detector. The result consists of grey-level edges with various strengths. Pseudo opening top-hat transformation is then applied to sharpen edge strengths. As edge strengths differ from regions, a recursive quad-tree decomposition scheme is adopted to threshold image into edge image in different regions. The overall implementation algorithm is illustrated in Fig. 4.

4.2. Formal presentation

As illustrated in Fig. 4, there are three steps involved in the proposed algorithm. Let I denote original image, B denote the structuring element in following discussions.

Step 1: *Morphological residue edge detection process*. Mathematical morphology dilation residue edge detector is applied to the image. Let I_e denote edge detected image, then

$$I_e = (I \oplus B) - I. \tag{11}$$

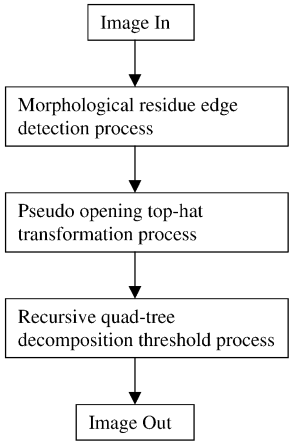

Fig. 4. Proposed algorithm to detect edges in dark regions as well as preserve feature edges in bright regions.

This image contains grey-level edges with various edge strengths. Some edges are sharp, some are smooth. If a global threshold value is applied everywhere, smooth edges are easily eliminated. To extract these smooth edge features, this image is processed by pseudo opening top-hat transformation.

Step 2: *Pseudo opening top-hat transformation process*. Pseudo opening top-hat transformation is applied in this process. Denoting invariant pixels set image as I_i, difference image set of I_e and I_i, denoted as I_p, is obtained:

$$I_p = I_e - I_i. \tag{12}$$

This image contains sharpened smooth edges in the presence of shading, as well as enhanced sharp edges. This process breaks the homogeneous characteristics of smooth background, leave it a sawtooth-like plane. This is solved by recursive quad-tree decomposition thresholding process.

Step 3: *Recursive quad-tree decomposition thresholding process*. Image I_p is decomposed into four subimages with same size, and each subimage is decomposed into four further, until the smallest size which is previously given has been reached. This is illustrated in Fig. 5.

To obtain a threshold value, mean and standard deviation in each $M \times N$ subimage are calculated as

$$\mu = \frac{1}{M \times N} \sum_{i=1}^{M} \sum_{j=1}^{N} I_{ij}, \tag{13}$$

$$\delta = \sqrt{\frac{1}{M \times N} \sum_{i=1}^{M} \sum_{j=1}^{N} (I_{ij} - \mu)^2}. \tag{14}$$

The threshold value is assigned as summation result of mean and standard deviation in each subimage. Meanwhile, global upper threshold bound and global lower threshold bound are set. As the summation result of global mean and standard deviation, the upper bound threshold value is set as the threshold value when the threshold value in each subimage is greater than this value. Similarly, as the subtraction result of global mean and standard deviation, the global lower threshold bound is set as the threshold value when the threshold value in each subimage is lower than this value. The global upper threshold bound is used to guide upper threshold value in order to extract sharp edges as much as possible. Similarly the global lower bound is used to guide lower threshold value in order to avoid extracting unnecessary small grey-level changes in background, which are usually not as much concerned as the objects in foreground. Additionally, in order to compensate the side-effect produced by pseudo opening top-hat transformation, a *homogeneous factor* is defined as the division of standard deviation by mean in each subimage:

$$H = \delta/\mu. \tag{15}$$

This equation is interpreted as 'roughness' of each subimage. In smooth background regions where homogeneous

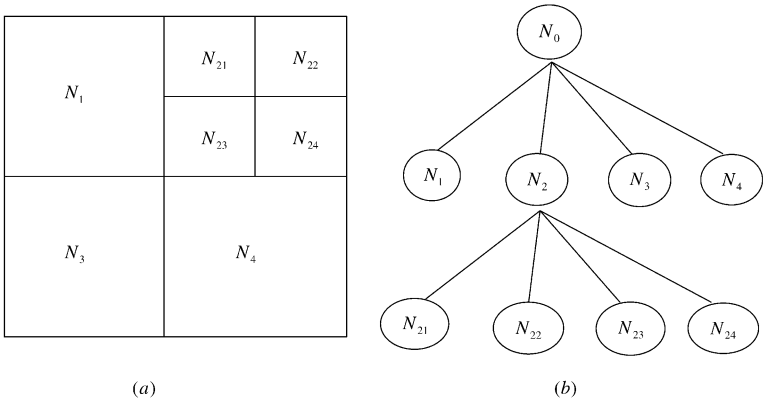

(a) (b)

Fig. 5. Illustration of quad-tree decomposition of image. (a) Quad-decomposition of image. (b) Quad-tree architecture.

characteristics are broken, the homogeneous factor is small, while in regions that contain sharp edges, the homogeneous factor is large. If the homogeneous factor of a subimage is lower than a given value, this subimage is regarded as part of smooth background, the maximum grey-level pixel value in this subimage is then set as threshold value to maintain homogeneous background region. This thresholding process is performed recursively, that is, four subimages are combined together as one subimage once each of them has been thresholded. This process ends when all subimages have been thresholded. This procedure is illustrated in Fig. 6.

5. Experiment result and analysis

In this section, the proposed PTHT edge detection algorithm is compared with a variety of existing methods for edge detection. Both synthetic images and natural scenes are used for comparison. The synthetic images use the Pratt's Figure of Merit as objective measure of performance, and the natural scene examines the applicability of these methods. Different noise distributions are used in experiment. The amplitude of the Gaussian noise is given in terms of signal-to-noise ratio (SNR) in dB,

$$\mathrm{SNR} = 20\log(10/\delta),$$

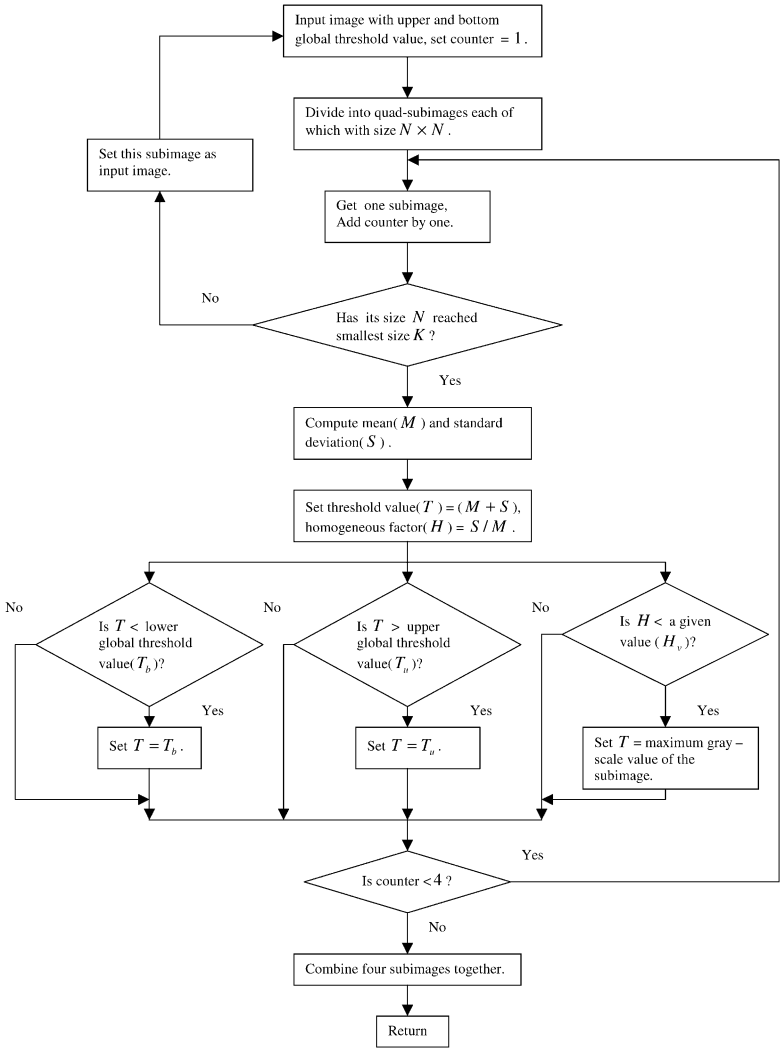

Fig. 6. Illustration of recursive quad-tree threshold of image.

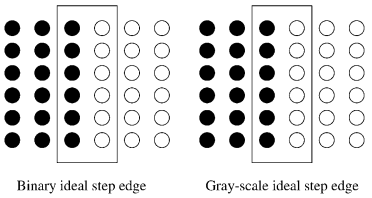

Fig. 7. Ideal step edges.

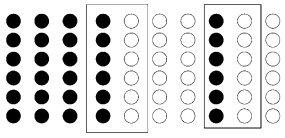

Fig. 8. Ideal step edge with step edge in dark region.

where 10 is the assumed edge height and δ^2 is the noise variance.

5.1. Synthetic images

The first experiment uses synthetic ideal step images since they allow objective performance measures. Two 8×8 synthetic images are composed of single vertical edge. One is in binary form, and the other is in grey scale form, which to the left of the edge, the grey level value is 8, to the right of the edge the grey level value is 0. The third one is a synthetic ideal step edge image with step edge in dark region. This is a typical type of edge simulated for comparing different edge detection methods for detecting edges in dark regions. They are illustrated in Figs. 7 and 8, respectively.

Pratt's figure of merit is a useful tool for quantitatively evaluating the performance of edge detectors. It is given by

$$R = \frac{100}{\max(N_I, N_D)} \sum_{i=1}^{N_D} \frac{1}{1 + \alpha d_i^2}, \tag{16}$$

where d_i is the distance between a pixel declared as an edge point and the nearest ideal edge pixel. The parameter α is a calibration constant and is chosen to be 1/9 for the results presented here. N_I and N_D represent the number of ideal edge points and detected edge points, respectively. A larger value R corresponds to better performance, with 100 being a perfect result.

Salt-and-pepper noise with noise density 0.03, 0.05, 0.07 and Gaussian noise with SNR 35, 37, 40 are added to these three ideal step edges, respectively. Lapalacian-of-Gaussian (Log), Sobel, Prewitt, difference of estimation (DoE) [8], pseudo top-hat transform (PTHT), morphological residue (MR), morphological blur-minimum residue (MBMR) edge detectors are applied to them, respectively. Figs. 9, 10 and 11 illustrate the results of applying Log, Sobel, Prewitt, DoE, PTHT, MR, MBMR edge detectors to ideal binary step edge under salt-and-pepper noise with different noise densities, respectively. It is shown that PTHT and MR edge detectors perform equally well under salt-and-pepper noise environment. Tables 1, 2 and 3 show the results of measured values of Pratt's Figure of Merit for different edge detectors under different noise distributions for different ideal step edges, respectively.

Table 1 illustrates the results of applying these edge detection methods to ideal binary step edge. The performance of Log, Sobel, Prewitt edge detectors are similar, as all of them are derivative edge detectors. It is shown that DoE edge detector is superior to derivative edge detectors. PTHT and MR edge detectors perform equally

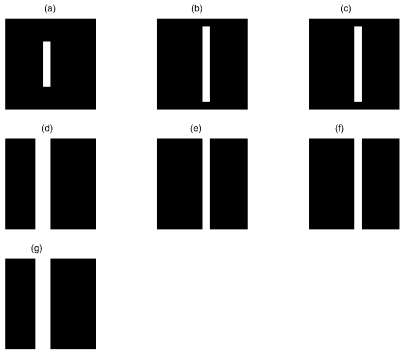

Fig. 9. The binary step edge detected by different edge detectors under salt-and-pepper noise with noise density 0.03. (a) Laplacian-of-Gaussian edge detector; (b) Sobel edge detector; (c) Prewitt edge detector; (d) DoE edge detector; (e) PTHT edge detector; (f) Morphological residue edge detector; (g) Morphological blur-minimum edge detector.

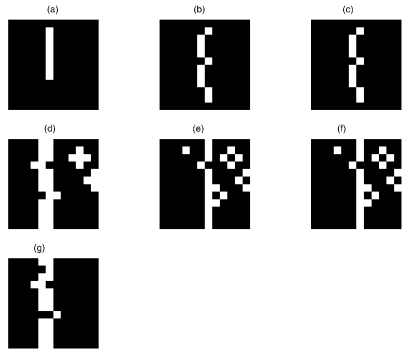

Fig. 10. The binary step edge detected by different edge detectors under salt-and-pepper noise with noise density 0.05. (a) Laplacian-of-Gaussian edge detector; (b) Sobel edge detector; (c) Prewitt edge detector; (d) DoE edge detector; (e) PTHT edge detector; (f) Morphological residue edge detector; (g) Morphological blur-minimum edge detector.

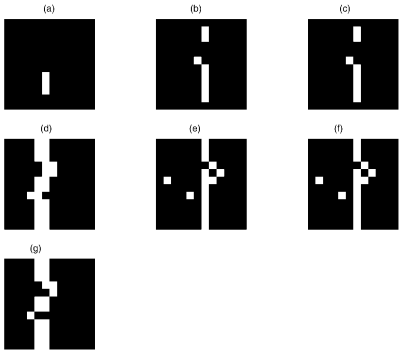

Fig. 11. The binary step edge detected by different edge detectors under salt-and-pepper noise with noise density 0.07. (a) Laplacian-of-Gaussian edge detector; (b) Sobel edge detector; (c) Prewitt edge detector; (d) DoE edge detector; (e) PTHT edge detector; (f) Morphological residue edge detector; (g) Morphological blur-minimum edge detector.

Table 1
The measured values of Pratt's Figure of Merit for a variety of different edge operators and noise distributions for binary ideal step edge

Edge detector	Noise distribution					
	SAP0.03	SAP0.05	SAP0.07	G35	G37	G40
Log	66.7	58.3	41.7	50	41.7	50
Sobel	75	75	67.5	60	45	60
Prewitt	75	75	67.5	52.5	45	60
DoE	90	90	82.5	60	60	75
PTHT	90	90	90	90	90	90
MR	90	90	90	90	90	90
MBMR	90	90	75	90	90	90

Table 2
The measured values of Pratt's Figure of Merit for a variety of different edge operators and noise distributions for grey-scale ideal step edge

Edge detector	Noise distribution					
	SAP0.03	SAP0.05	SAP0.07	G35	G37	G40
Log	50	58.3	50	50	50	50
Sobel	52.5	52.5	75	50	52.5	50
Prewitt	52.5	52.5	75	58.3	52.5	58.3
DoE	82.5	82.5	90	52.5	82.5	75
PTHT	90	90	90	90	90	90
MR	90	82.5	90	90	90	90
MBMR	90	90	75	90	90	90

well, so does MBMR edge detector, under different Gaussian noise distributions. Table 2 shows the results of applying these edge detection methods to ideal grey-scale step edge. Log, Sobel, and Prewitt edge detectors perform similarly, though worse than DoE edge detector. PTHT, MR and MBMR edge detectors obtain similar results. The results of applying different edge detectors to detect ideal step edge with step edge in dark region are shown in Table 3. The pair number indicates the measured value of Pratt's Figure of Merit for ideal step edge with step edge in dark region respectively. It is shown that Log edge detector performs worse than DoE edge detector. PTHT and MR edge detectors provide equally satisfactory performance. MBMR edge detector performs well under salt-and-pepper noise distributions with 0.03, 0.05, though worse than PTHT edge detector under different Gaussian noise distributions.

Table 3
The measured values of Pratt's Figure of Merit for a variety of different edge operators and noise distributions for ideal step edge with step edge in dark region

Edge detector	Noise distribution					
	SAP0.03	SAP0.05	SAP0.07	G35	G37	G40
Log	33.3, 0	33.3, 0	16.7, 0	16.7, 0	0, 0	25, 0
DoE	90, 0	90, 0	90, 0	25, 82.5	25, 75	45, 67.5
PTHT	90, 90	90, 90	90, 90	90, 90	90, 90	90, 90
MR	90, 90	90, 90	90, 90	90, 90	90, 90	90, 90
MBMR	90, 0	90, 0	82.5, 0	90, 52.5	90, 67.5	90, 75

The nonlinear prefilters discussed in Ref. [9], such as the lower-upper-middle (LUM), comparison and selection (CS) and weighted majority of samples with minimum range (WMMR) prefilters, are also applied to these three ideal step edges. Comparison results are presented in Tables 4, 5 and 6, respectively. As shown in these tables, the measured values of Pratt's Figure of Merit are all zeroes, obtained from LUM, CS or WMMR prefilters and Sobel edge detector, under different noise distributions, which fail to extract ideal binary/grey-scale step edge and ideal step edge with step edge in dark region. However, PTHT edge detector performs well in this task.

5.2. Natural scenes

Experiments are performed on a picture of cameraman. As shown in Fig. 12, cameraman wears a black coat, on which it is too dark to see any details in shading part of the coat by human eyes. If this image is enhanced as Fig. 13, it shows clearly the edge features of pocket, buttons and hands in the dark regions of the coat.

For comparison purpose, classical Sobel edge detector, mathematical morphological residue edge detector, DoE edge detector, Lum prefilter followed by Sobel edge detector are applied on this image. The experiment results are shown as in Figs. 14, 15, 16, and 17, respectively.

Table 4
The measured values of Pratt's Figure of Merit for Lum, Cs, Wmmr prefilter and noise distributions for binary ideal step edge

Edge detector	Noise distribution					
	SAP0.03	SAP0.05	SAP0.07	G35	G37	G40
Lum prefilter followed by Sobel	0	0	0	0	0	0
Cs prefilter followed by Sobel	0	0	0	0	0	0
Wmmr prefilter followed by Sobel	0	0	0	0	0	0
PTHT	90	82.5	82.5	90	90	90

Table 5
The measured values of Pratt's Figure of Merit for Lum, Cs, Wmmr prefilter followed by Sobel edge detector under different noise distributions for grey-scale ideal step edge

Edge detector	Noise distribution					
	SAP0.03	SAP0.05	SAP0.07	G35	G37	G40
Lum prefilter followed by Sobel	0	0	0	0	0	0
Cs prefilter followed by Sobel	0	0	0	0	0	0
Wmmr prefilter followed by Sobel	0	0	0	0	0	0
PTHT	90	90	90	90	90	90

Table 6
The measured values of Pratt's Figure of Merit for Lum, Cs, Wmmr prefilter followed by Sobel edge detector under different noise distributions for ideal step edge with step edge in dark region

Edge detector	Noise distribution					
	SAP0.03	SAP0.05	SAP0.07	G35	G37	G40
Lum prefilter followed by Sobel	0, 0	0, 0	0, 0	0, 0	0, 0	0, 0
Cs prefilter followed by Sobel	0, 0	0, 0	0, 0	0, 0	0, 0	0, 0
Wmmr prefilter followed by Sobel	0, 0	0, 0	0, 0	0, 0	0, 0	0, 0
PTHT	90, 90	90, 90	67.5, 90	82.5, 90	90, 90	90, 90

Fig. 12. Picture of a cameraman.

Fig. 13. Picture of enhanced cameraman.

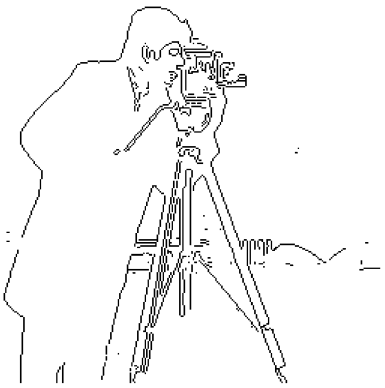

Fig. 14. Cameraman processed by Sobel.

Fig. 15. Cameraman processed by Morphological residue.

Fig. 16. Cameraman processed by DoE.

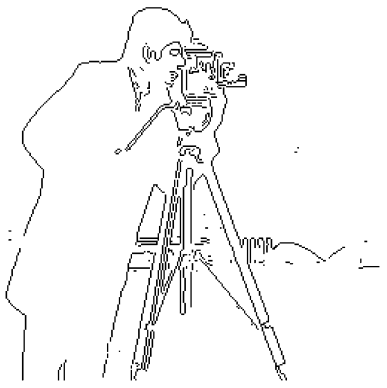

Fig. 17. Cameraman processed by Lum prefilter followed by Sobel.

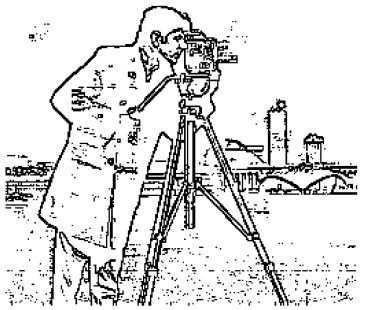

Fig. 18. Cameraman processed by PTHT.

Table 7
The computation and memory requirements of PTHT algorithm for an $N \times N$ image

PTHT	Computation time	Memory(Bits)
Step 1	$O(N^2)$	$16N^2$
Step 2	$O(1)$	$16N^2$
Step 3	$O(N^2/Ns^2)$	$(4^0 \times (N \times N) + 4^1 \times (N/2 \times N/2) + \cdots + 4^n \times (N/Ns \times N/Ns)) * 8$
Total	$O(N^2) + O(N^2/Ns^2)$	$32N^2 + (4^0 \times (N \times N) + 4^1 \times (N/2 \times N/2) + \cdots + 4^n \times (N/Ns \times N/Ns)) * 8$

Sobel edge detector, morphological residue edge detector detect contour of cameraman successfully, but fail to extract contour of tower. DoE edge detector detects contour of cameraman only, fails to detect contour of tower, and edge features of cameraman in dark regions are lost. Lum prefilter followed by Sobel edge detector extracts contour of cameraman only and fails to detect contour of tower. It is shown in Fig. 18 that proposed PTHT edge detection algorithm detects the contour of cameraman, extracts contour of tower as well as extracts edge features in dark regions on the coat of cameraman successfully.

Table 8
The computation and memory requirements of stacking filtering algorithm for an $N \times N$ window (all stack filters were trained using 10 passes of the training algorithm)

	Table lookups per pixel	Swaps per pixel	Memory(Bits)
Filtering	N^2	N/A	2^{N^2}
Training	N^2	$< N^4$	2^{N^2+3}
Total	$11N^2$	$< 10*(N^4)$	$2^{N^2} + 10*2^{N^2+3}$

6. Computation time and memory requirements

The computation time and memory requirements of PTHT edge detection algorithm for $N \times N$ images are listed in Table 7, in which Ns is subimage size. As there are three steps involved in PTHT edge detection algorithm, the computation and memory requirements of each step are listed, respectively. For morphological residue edge detection process, for an $N \times N$ image, morphological residue edge detection requires to store two images, one is dilated image and the other is original one, thus it requires $2N^2*8$ bits computer memory. Morphological dilation process consists of two for-loops, they require $O(N^2)$ computation time, while the assignment operation which takes $O(1)$ time can be ignored. For pseudo opening top-hat transformation, it involves two images, one is invariant pixels set image, the other is the result image from former step, thus it requires $2N^2*8$ bits computer memory. The operation is simply assignment operation that takes $O(1)$ computation time. For recursive quad-tree decomposition threshold process, image is divided into four subimages, each of which is $Ns \times Ns$. The final total numbers of subimages are N^2/Ns^2. Assume $n = \log_4(N^2/Ns^2)$, to split image into this final number, it requires $4^0 + 4^1 + \cdots + 4^{n-1}$ times which are approximately $O(N^2/Ns^2)$ computation time. In each image splitting process, it is simply assignment operation which takes $O(1)$ computation time, which is much less than splitting times that can be ignored. For memory requirement, it requires $(4^0 \times (N \times N) + 4^1 \times (N/2 \times N/2) + \cdots + 4^n \times (N/Ns \times N/Ns))*8$ bits memory. For comparison purpose, the computation time and memory requirements of stack filtering, which is the core part of implementation of DoE edge detector, are listed in Table 8. For a size 256×256 image, assume that Ns equals 16, memory requirement for PTHT edge detection algorithm is 2.3 MB. For the stacking filtering algorithm, for a size 256×256 image, and a 5×5 window, the memory requirement is 324 MB.

7. Conclusion

A novel mathematical morphology edge detection algorithm to detect smooth edge features in dark regions in image has been presented. Pseudo top-hat morphological transformation, stemmed from top-hat morphological transformation, is defined to distinguish small grey-level changes in dark regions. A recursive quad-tree decomposition scheme is also proposed to threshold grey-level edge image to binary edge image. Comprehensive comparison experiments have been carried out on synthetic and natural scene images. Experimental results show that PTHT edge detection algorithm outperforms other edge detection methods on retrieving smooth edge features in dark regions while preserving boundary of objects successfully. Selecting appropriate illumination is an important aspect for machine vision system design. However, this edge detection algorithm has provided an efficient solution to machine vision applications, when lighting is not evenly distributed on objects inspected. The ambient illumination, such as controlled frontal illumination and backlighting illumination, is adequate for the cases investigated using the proposed technique which is not sensitive to the range of lighting conditions.

References

[1] B. Chanda, M.K. Kundu, Y.V. Padmaja, A multi-scale morphologic edge detector, Pattern Recognition 31 (10) (1998) 1469–1478.
[2] V.S. Nalwa, A guided tour of computer vision, AT&T Bell Laboratories, 1993.
[3] R.C. Gonzalez, P. Wintz, Digital Image Processing, Addison-Wesley, England, 1992.
[4] J. Serra, Image Analysis and Mathematical Morphology, Academic Press, New York, 1982.
[5] J.S.J. Lee, R.M. Haralick, L.G. Shapiro, Morphological edge detection, IEEE J. Robot. Automat. RA-3 (2) (1987) 142–156.
[6] R.J. Feehs, G.R. Arce, Multidimensional morphological edge detection, SPIE, Visual Commun. Image Process. II 845 (1987) 285–292.
[7] J.R. Parker, Algorithms for Image Processing and Computer Vision, Wiley Computer, New York, 1997.
[8] J. Yoo, C.A. Bouman, E.J. Delp, E.J. Coyle, The nonlinear prefiltering and difference of estimates approaches to edge detection, CVGIP: Graph. Models Image Process. (1993) 140–159.
[9] R.C. Hardie, C.G. Boncelet, Gradient-based edge detection using nonlinear edge enhancing prefilters, IEEE Trans. Image Process. (1995) 1572–1577.

About the Author—TING CHEN graduated from Shenzhen University, China, in 1994 and obtained her B.Sc. degree in Electrical Engineering from Shenzhen University. From 1994 to 1997, she worked as a software engineer in Software Technology Center of Industrial and Commercial Bank of China (ICBC). Now she is a Ph.D. student in Department of Electrical Engineering and Electronics, The University of Liverpool, UK.

About the Author—HENRY WU graduated from Huazhong University of Science and Technology (HUST), China, in 1978 and obtained an M.Sc.(Eng) degree in Electrical Engineering from HUST in 1981. From 1981 to 1984, he was appointed Lecturer in Electrical Engineering in the University. He obtained a Ph.D. degree from The Queen's University of Belfast (QUB) in 1987. He worked as a Research Fellow and Senior Research Fellow in QUB from 1987 to 1991 and as Lecturer and Senior Lecturer in the Department of Mathematical Sciences, Loughborough University of Technology, UK from 1991 to 1995. He is a Royal Chartered Engineer and Fellow of IEE and also a Senior Member of IEEE. Presently he holds the Chair of Electrical Engineering in the Department of Electrical Engineering and Electronics, The University of Liverpool, UK, acting as the Head of Intelligence Engineering and Automation group. Professor Wu's research interests include adaptive control, neural networks, learning systems, evolutionary computation, information processing and extraction, power system control and operation.

About the Author—REZA RAHMANI-TORKAMAN is a graduate from Coventry University, and holds a Masters degree from UMIST. He has amassed over 17 years experience working within manufacturing industry, much of that time being involved in the development of manufacturing systems. He has supervised several image processing application. His current position is that of Departmental Manager, Manufacturing Systems Engineering (MSE), BICC General UK Cables Ltd at Wrexham, which provides cable manufacturing systems to BICC General world-wide.

About the Author—JIM HUGHES holds an honours degree in Electrical Engineering from Liverpool University, plus a post-graduate diploma in Manufacturing—Management and Technology. He has over 20 years experience in a variety of engineering roles within manufacturing industry, including industrial and graphic design and project management. He presently heads the Applications Engineering Team at MSE in Wrexham, responsible for manufacturing systems implementation projects in BICC/General cable-making factories around the world.